Tribology International 168 (2022) 107437

Contents lists available at ScienceDirect

Tribology International

journal homepage: www.elsevier.com/locate/triboint

Optimizing the Mo concentration in low viscosity fully formulated oils

Aaron Thornley [a], Yuechang Wang [a,*], Chun Wang [a], Jiaqi Chen [b], Haipeng Huang [b], Hong Liu [b,*], Anne Neville [a], Ardian Morina [a]

[a] Institute of Functional Surfaces, School of Mechanical Engineering, University of Leeds, Leeds LS2 9JT, UK
[b] Sinopec Lubricant Co., Ltd., Beijing 100085, China

ARTICLE INFO

Keywords:
Molybdenum dithiocarbamate
Film thickness
Low viscosity engine oils
Tribofilm chemistry

ABSTRACT

Molybdenum dithiocarbamate (MoDTC) is usually added in low viscosity engine oils to improve its ability to reduce friction. However, increasing the amount of MoDTC added results in unwanted sulfated ash increases and other adverse effects. Thus, it is necessary to investigate the optimization of the amount of MoDTC added. The current work investigates this topic in terms of the Mo concentration in the lubricant. Seven different Mo concentrations with the same additive package are tested, whose tribological properties and chemistry of the tribofilm are investigated. For the selected operating conditions in this study, the critical concentration of Mo is determined to be ≈ 350 ppm due to its ability to reduce the friction to ≈ 0.04 under a constant and varying lambda ratio by forming the required threshold thickness of MoS_2 within the tribofilm matrix, dominated by zinc dialkyl dithiophosphate (ZDDP) species. In general, increasing the Mo concentration increases the formation rate of MoS_2 in the initial stages of the traction, directly forming a thicker MoS_2 layer within the tribofilm up to a specific Mo concentration. Induction time also decreases with increasing Mo concentration, and increasing the Mo concentration from 350 to 1000 ppm does not negatively impact the wear generated.

1. Introduction

Original equipment manufacturers (OEMs) are constantly finding new ways to increase the fuel economy for their vehicles. Such drive for better fuel economy has been increased due to strict CO_2 emissions legislation from countries and regions such as China and Europe [1–3]. Therefore, OEMs have to implement different solutions to meet these requirements set by international governments.

One efficient approach to increase the fuel economy that OEMs are taking is to decrease the viscosity of the engine oil. Previous research has shown that a 2.75% fuel efficiency increase can be achieved using an SAE 5 W-20 oil compared to an SAE 10 W-30 oil [4]. Lowering the viscosity further still produces positive results; a 1.5% increase can be achieved using a 0 W-20 compared to a 5 W-30 [5]. A new oil grade has been introduced recently as SAE 0 W-8 to counteract the tighter CO_2 reductions further. Since this is a relatively new oil grade, little research has been conducted on 0 W-8 engine oils. It must be noted that there are multiple differing fuel economy tests and engines using ultra-low viscosity engine oil to which the results have not always provided a positive result [6]. However, recent studies have shown that a fuel economy increase of 0.57% and 0.8% can be obtained using a 0 W-8 engine oil compared to 0 W-16 [7,8].

There are several advantages of using low viscosity oils. Decreasing the viscosity of the oil improves the pumping ability during cold starts. In addition, it enables the oil to be thin enough to lubricate the components upon engine start-up, ensuring the least amount of time it takes to complete an entire cycle of lubrication within the ICE. All the contacts of moving parts under lubrication travel through different lubrication regimes during operation. A graph of the main lubricated components of an ICE with the regimes they operate in is shown in Fig. 1-1. The Stribeck curve is utilized to visualize the overall view of friction variation in the different lubrication regimes. Boundary lubrication means more metal-on-metal contacts and increased friction, whereas hydrodynamic regime means total separation of the surfaces through lubrication and reduced friction. In terms of friction, previous research has shown that lowering the oil viscosity decreases the hydrodynamic friction in the bearings and other components [9]. However, lowering the viscosity of the lubricating oil also shifts all the components' lubrication regimes towards the boundary regime, decreasing the tribo-contact lambda ratios.

* Corresponding authors.
E-mail addresses: mnatho@leeds.ac.uk (A. Thornley), y.wang1@leeds.ac.uk (Y. Wang), c.wang@leeds.ac.uk (C. Wang), chenjq776.lube@sinopec.com (J. Chen), huanghp.lube@sinopec.com (H. Huang), liuh.lube@sinopec.com (H. Liu), a.neville@leeds.ac.uk (A. Neville), a.morina@leeds.ac.uk (A. Morina).

https://doi.org/10.1016/j.triboint.2022.107437
Received 4 December 2021; Received in revised form 10 January 2022; Accepted 11 January 2022
Available online 14 January 2022

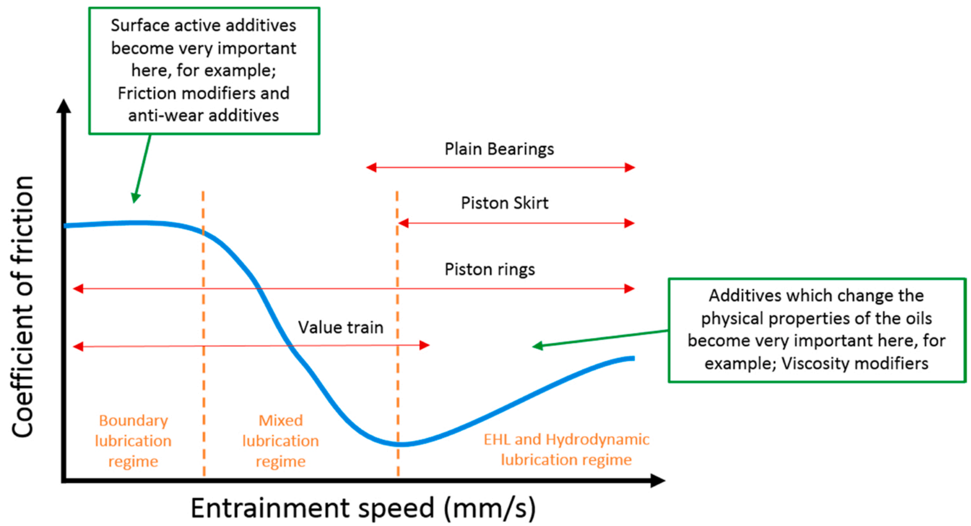

Fig. 1-1. Lubrication regime Stribeck curve of the internal combustion engine components.

Decreasing oil viscosity generates more metal-to-metal contact between the components, especially at high temperatures where the oil is at its thinnest [10]. In addition, components that make up the piston assembly, exhaust, and inlet valve all have increased friction when lowering the oil's viscosity, as these operate at lower lambda ratios. Therefore, boundary-active additives such as MoDTC and ZDDP become more important as the oil's viscosity is lowered to ensure low friction and wear [11–14].

The increased fuel economy demands are causing countries like Japan to increase the concentration of MoDTC to very high amounts of 1000 + ppm, which supposedly gives prolonged fuel economy boosts. However, when lowering the oil's viscosity, the concentration of boundary additives has to be increased due to a decrease in lambda ratio at the tribo-contacts and additive depletion due to oxidation [15]. In addition, there is also a need to reduce the amount of sulfur, which is part of the MoDTC molecule within engine oils due to its harmful effects on the engine and its relatively high cost [16,17]. Therefore, understanding the behavior of MoDTC in fresh oils and aged oils is extremely important, which will directly lead to the optimization of MoDTC.

The Mo concentration for new ultra-low viscosity engine oils must be optimized to ensure low friction is achieved over a long oil drain interval (ODI). The friction modifier must perform in the harsher conditions created by lowering the oil viscosity. However, it does not need to be present in great excess such that it is expensive/inefficient and a significant contributor to harmful products. To investigate the optimum Mo concentration for the new ultra-low fully formulated engine oils, specific criteria have to be analyzed. The first is Friction reduction, which has a massive influence on the fuel economy of the ICE. The fuel economy will be negatively impacted if the concentration is too low to produce friction reduction and low steady-state friction. Since most OEMs increase the Mo concentration to closer to 1000 ppm, the impact on the tribofilm must be understood. The increase of Mo concentration could potentially reduce the ZDDP products found within the tribofilm known for their anti-wear properties. Finally, the impact of increasing the Mo concentration has on wear has to be investigated. The optimum Mo concentration must not negatively impact the wear or friction while keeping a higher fuel economy than the higher viscosity oil counterparts.

2. Experimental procedures

2.1. Test oils

A fully formulated 0 W-8 engine oil with no friction modifier provided by Sinopec has been used as the base fluid. Six different Mo concentrations were added to the base fluid to assess their tribological performances.

The seven formulations tested in this study are shown in Table 2–1. All the sample oil's kinematic viscosities are within the 0 W-8 engine oil grade bracket according to the American Society for Testing and Materials (ASTM) D445. High-temperature high shear viscosities (HTHS) and cold cranking simulator (CCS) were performed by Sinopec Lubrication Company according to ASTM D4683 and D5293 standards.

Inductively Coupled Plasma Mass Spectroscopy (ICP-AES) was used to measure the concentration of Mo within the sample oils and the other elements associated with the other additives within the fully formulated oils. As expected, elements associated with ZDDP and the detergents such as Zn, P, and Ca all had similar values in the sample oils. The only different elements in the sample oils are Mo and S, both associated with the structure of MoDTC. Such simultaneous variations in both S and Mo might dilute the optimization Mo concentration found in the current study. However, the increase of S is inevitable as increasing Mo concentration by adding MoDTC. We chose MoDTC as it is widely used in commercial engine oil to introduce Mo. It should also be noted that the ability of the Mo element to reduce friction is achieved through forming MoS_2. Thus, the S element must be included in the lubricant. Therefore, although the simultaneous variations in both S and Mo have adverse effects on the optimization of Mo concentration, the outcome of this paper is still practical and can be used in developing low viscosity engine oil. In future studies, lubricants with only Mo concentration varying should be investigated.

Table 2-1
Test oil formulations.

Sample number	1	2	3	4	5	6	7
KV 100/D445	5.34						
KV 40D445	25.46						
HTHS 150/D4683	1.92–1.94						
CCS 35/D5293	3550						
Mo conc. (ppm)	0	85	180	350	500	750	1000
S conc. (ppm)	2976	3200	3309	3614	4349	4544	5059

2.2. Tribological testing

2.2.1. Friction

To measure the friction and tribofilm growth under certain operating conditions, an MTM and spacer layer imaging (SLIM) camera was used. The schematic for the MTM is shown in Fig. 2-1. An AISI 52100 steel alloy ball, 19.05 mm in diameter, is loaded against a flat AISI 52100 steel alloy disc, 46 mm in diameter, submerged in the oil sample, ≈ 35 mL. The contact orientation is a ball on disc which are independently driven to create the required conditions. Before the experiments began, both the ball and disc were cleaned in methanol using an ultrasonicating bath for 5–10 min. This is to prevent any contamination affecting the performance of the oil and results obtained.

To understand the influence of Mo concentration when the contact is under a constant lambda ratio and a rapidly varying lambda ratio, two steps were used in the experiment: Stribeck and traction. A schematic of the MTM test procedure is shown in Fig. 2-2. The test starts and ends with a mapper step. In the Stribeck phase, the parameters kept constant are temperature, slide to roll ratio (SRR), load, and contact pressure, with the entrainment speed being the only criterion that changes. Entrainment speed decreases from 2000 mm/s to 10 mm/s to protect any tribofilm that forms during the traction phase by avoiding the low lambda ratio at the beginning of the phase [18]. In the traction phase, all parameters, such as temperature and load, are kept constant. Entrainment speed is fixed at 100 mm/s, corresponding to a typical lambda ratio value of 0.2 found in the ICE [19].

Lambda ratios for a known speed were calculated using the Dowson & Higginson minimum thickness for a point contact equation as shown in Eqs. 1 and 2. The operating conditions and materials used in the MTM tests are shown in Table 2-2, with surface roughnesses of the ball and disc being < 0.02 μm Ra. The SRR is defined as $(U_B\text{-}U_D)/U$ where the sliding speed is $U_B\text{-}U_D$ and entrainment speed or mean rolling speed is

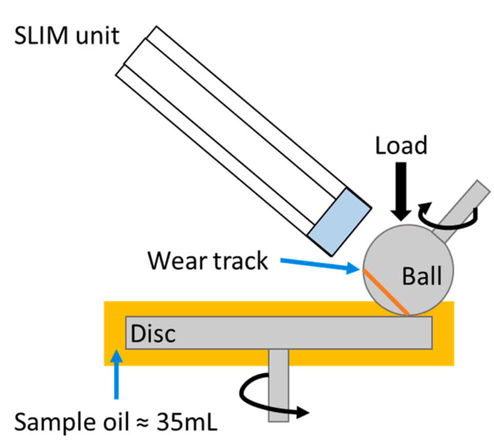

Fig. 2-1. MTM schematic.

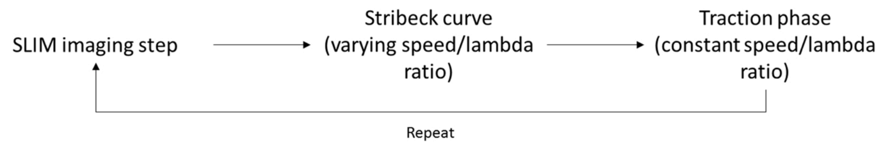

Fig. 2-2. MTM test procedure.

Table 2-2
MTM operating conditions.

Parameters	Stribeck curve phase	Traction phase
Materials	AISI 52100 Steel ball and disc	AISI 52100 Steel ball and disc
Sliding rolling ratio % (SRR)	100	100
Load (N)	40	40
Hertzian/contact pressure (GPa)	1.0	1.0
Speed (mm/s)	2000 ~ 10	100
Temperature (°C)	120	120

$U = (U_B + U_D)/2$. In total, there are 8 Stribeck phases and eight traction phases. Stribeck curves were taken at intervals of 0, 5, 60, 240, 480, 720, 960, and 1200 min of traction. The total running time of the test is 24 h. This test duration was chosen to understand the amount of the MoDTC depleted within the tribo-contact during the test with harsh operating conditions.

$$\frac{h_{min}}{R^*} = 3.63\left(\frac{U\eta_0}{E^*R^*}\right)^{0.68}(\alpha E)^{0.49}\left(\frac{W}{E^*R^*}\right)^{-0.073}\left(1-e^{-0.68k}\right) \quad (1)$$

$$\lambda = \frac{h_{min}}{\sum R_a} \quad (2)$$

2.2.2. *Optical film thickness*

Experiments of selected sample oils were conducted with the additional SLIM technique to obtain the tests' optical film thickness and repeatability. A schematic of the optical interference technique is shown in Fig. 2-3.

MoDTC in a binary system does not produce a tribofilm where the optical film thickness can be measured accurately [20]. In some cases, the steady-state thickness is < 10 nm or produces an extremely small value [20]. Previous research has shown the SLIM technique to accurately measure the ZDDP/phosphate glass films and not MoDTC/MoS_2 films [21–23]. Therefore, for this research, the influence of MoDTC and its concentration has on the ZDDP film formation can be investigated.

During the test to obtain the SLIM images, the ball is unloaded from the disc and loaded against a thin Cr layer coated glass disc. White light

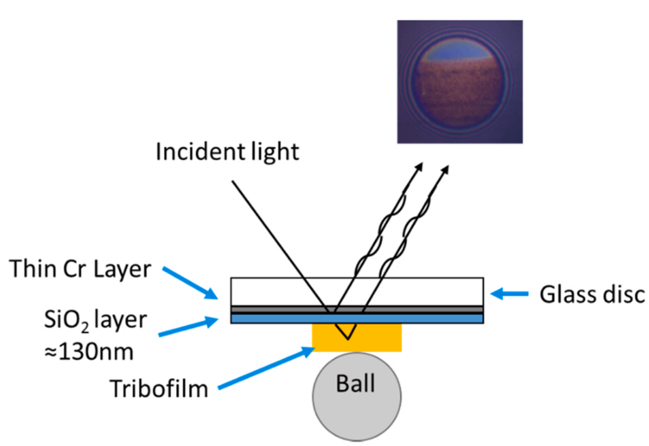

Fig. 2-3. SLIM technique.

is then illuminated down a microscope, and an image of the tribofilm is taken. The ball is then reloaded onto the disc, and the next step begins. This process is repeated at every interval previously stated. The repeat test duration was changed to 4 hrs, with SLIM measurements obtained at intervals of 0, 5, 15, 30, 60, 120, 180, and 240 min.

2.3. *Surface analysis*

Before any surface analysis technique was performed, the ball was cleaned with heptane to remove any potential excess oil left on the samples after MTM testing.

2.3.1. *X-ray Photoelectron Spectroscopy*

Chemical analysis of the tribofilm was conducted using XPS. The X-ray source was Al Kα 1486.6 eV, with two types of scans used in the XPS analysis: High resolution (HR) and survey scans. In addition, etching was also utilized to understand the compounds and element weight % in the different layers of the tribofilms. The etching was performed using an Ar^+ ion beam at 2 keV with a sputtering current of 1 uA. Previous literature has shown that this setting produces an etch rate on steel of 4.5 nm per minute by Wyko [24].

Survey scans were performed to identify the elements present within the area of interest. The chemical composition of the tribofilms was obtained by performing HR scans. Mo 3d curve fitting was conducted using certain conditions and constraints. The area peak ratio of $3d_{5/2}$: $3d_{3/2}$ is always equal to 3:2. In contrast, the binding energy difference between the two spin orbitals is always a constraint to 3.13 eV [25].

The C1s signal for calibration due to potential charging during acquisition is set to 285 eV before any analysis is undertaken [26]. Shirley line type was used as a standard baseline, and different line shapes were used for the peaks to distinguish the different components within the signals.

2.3.2. *Raman spectroscopy*

Reinshaw Raman spectrometer system has been used to obtain MoS_2 tribofilm distribution on the wear scar. Raman spectra for all tribofilms generated on the balls were obtained with a 488 nm wavelength laser with a 10% power filter, 10 s exposure time, and two accumulations per acquisition. Power filter at 10%, low exposure time of 10 s, and two accumulations were selected to prevent the laser from damaging the tribofilm. The 488 nm wavelength laser was selected as previous research has shown it is critical for MoS_2 tribofilm detection [27].

A mapping area of 100 µm x 100 µm with a step of 7 µm x 7 µm was obtained from the middle of the wear scar, which equates to 225 points taken in total. An example of the Raman spectra where MoS_2 is detected is shown in Fig. 2-4 and the peaks and associated vibration modes. The vibration modes E_{2g} wavelength number is ≈ 381 cm^{-1}, and A_{1g} is ≈ 408 cm^{-1}. Raman intensity maps were generated using the A_{1g} peak intensities [28]. Scale bars for the A_{1g} peak intensities were kept the same to enable comparisons.

2.4. *Wear analysis*

Wear analysis of the samples was conducted on the discs using an NPFlex, utilizing the white light interferometer technique. The majority of the tribofilm was initially removed before obtaining images for analysis. Tribofilm removal was conducted using a 0.05 M EDTA solution applied to the wear track for 1 min [29]. Due to the contact being

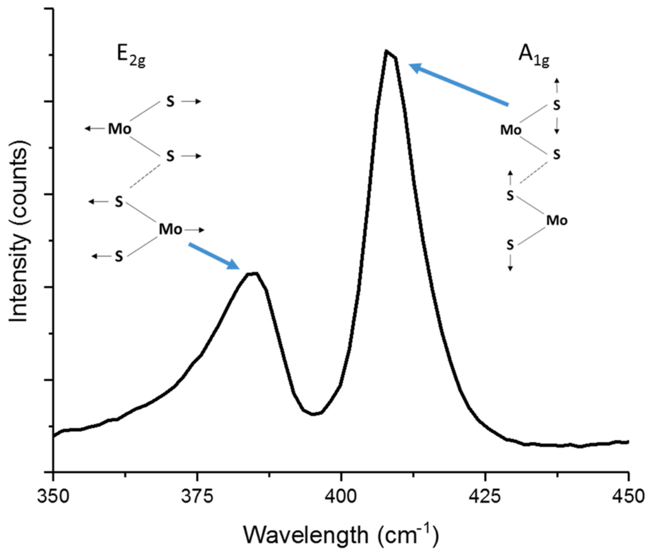

Fig. 2-4. Spectra example with the vibration nodes associated with MoS_2.

unidirectional and the wear scar not concentrated in a straight line, three areas of interest on the discs were chosen for analysis using the NPFlex, as shown in Fig. 2-5. Averages of the wear volume loss, $V_{wear\ volume\ loss}$ is then taken from these three areas to calculate the wear coefficient, K, using the Archard expression shown in Eq. 3, where L is sliding distance and W is load.

$$K = \frac{V_{wear \quad volume \quad loss}}{LW} \tag{3}$$

3. Results and discussion

3.1. Friction analysis

Friction is the most important factor when investigating the critical and optimum Mo concentration within a selection of engine oils. Two aspects of friction, steady-state and Stribeck curve, from the MTM results, can be used to help understand how Mo concentration changes influence the coefficient of friction values during operation. Steady-state friction is the friction value under a constant speed and lambda ratio. In contrast, Stribeck curve friction is when the contact is under a varying entrainment speed and lambda ratio.

3.1.1. Steady-state coefficient of friction

Fig. 3-1 displays the coefficient of friction vs. time graph for all the sample oils for the first 3000 s during the traction phase at a constant speed, while Fig. 3-2 shows the final 3600 s of traction to end the 24 h

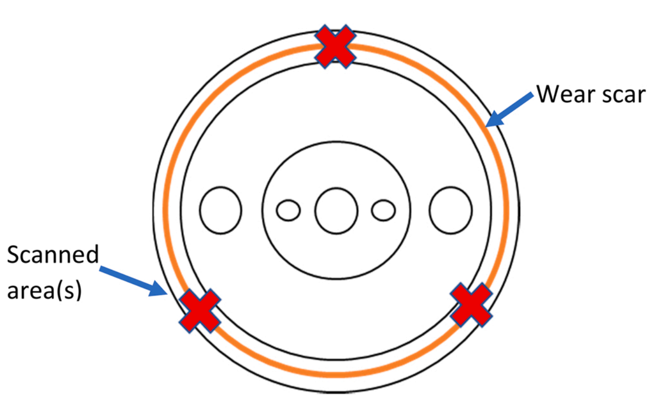

Fig. 2-5. Selected areas of analysis.

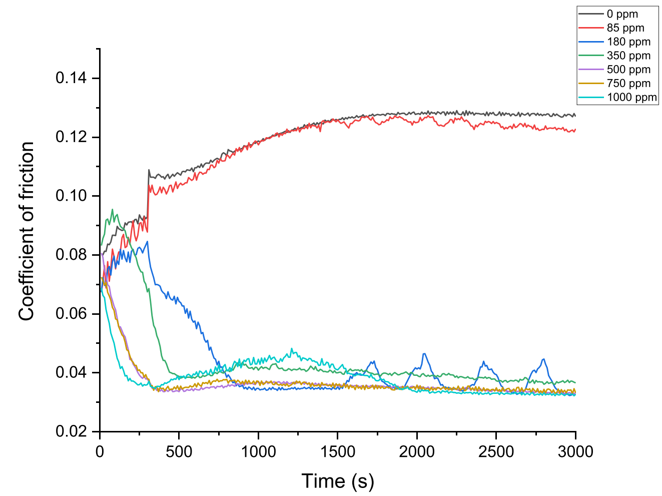

Fig. 3-1. First 3000 s in the traction phase at a constant speed for all Mo concentrations.

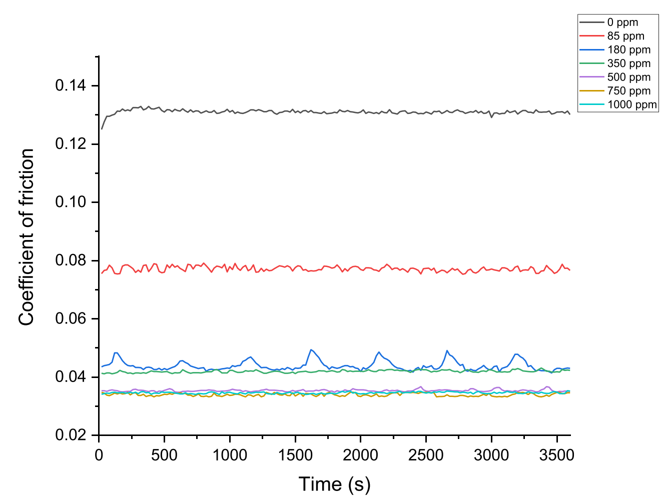

Fig. 3-2. Final 3600 s of the 24 h of traction for all Mo concentrations.

test. Fig. 3-1 highlights the induction friction, and Fig. 3-2 the steady-state friction for all the Mo concentrations.

It is clear from Fig. 3-1 that all concentrations $\geq$ 180 ppm reduce the friction coefficient to $\approx$ 0.04 in the traction phase. A general trend of increasing Mo concentration to reduce the friction induction time is also observed, and the theory behind this is discussed in the later sections. The friction induction periods are typical of MoDTC in fully formulated or formulated with base oils from previous research, where a sharp drop is observed due to MoS_2 formation within the tribofilm matrix [30–32]. Towards the end of the 24 h of traction, all Mo concentrations are at their steady-state friction values, as shown in Fig. 3-2. However, 180 ppm of Mo's friction fluctuates a lot more than the other concentrations. Again, the theory behind this is discussed in the later sections.

The steady-state coefficient of friction values from the traction phase for the range of Mo concentrations tested on the MTM is shown in Fig. 3-3. These values are calculated by taking the average friction for each concentration towards the end of the traction phase as shown in Fig. 3-2.

The sample oil with no Mo concentration as expected produces a high coefficient of friction value. This value is typical of oils that do not contain a friction modifier with a tribofilm containing anti-wear and detergent additives [33]. As the Mo concentration is increased to 85 ppm, a drop in steady-state friction is observed from $\approx$ 0.14 to $\approx$ 0.08. However, the friction reduction is only $\approx$ 0.08 and not the

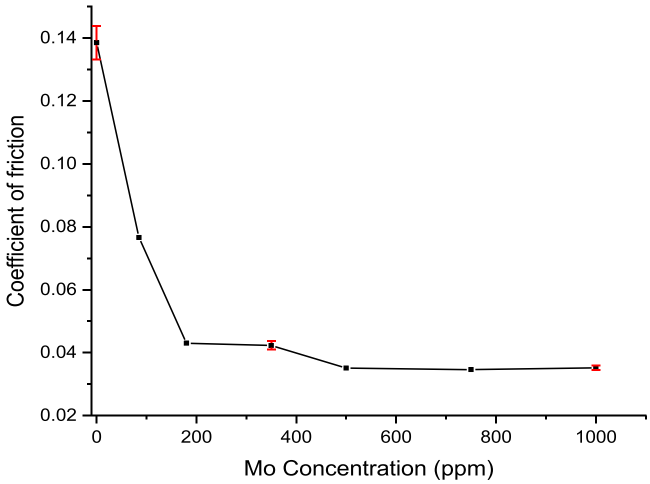

Fig. 3-3. Steady-state friction for all Mo concentrations.

typical value of ≈ 0.04 expected from a MoS_2 rich tribofilm. Thus, 85 ppm of Mo provides a sufficient concentration to reduce friction but not enough to generate the ≈ 0.04 friction value.

This paper's minimum Mo concentration, which produces a steady-state friction value of ≈ 0.04 in the traction phase at a constant lambda ratio, is 180 ppm. The concentration chosen is only based on the friction under a constant lambda ratio, and it must keep the friction under varying lambda ratios in the boundary and mixed regimes. However, it must be noted that no concentration between 85 and 180 ppm of Mo was tested, and the minimum concentration could be within the upper limit of the range between them. All concentrations greater than 180 ppm all produced steady-state friction values ≈ 0.04. Research has shown that the critical concentration within a binary system of base oil and MoDTC with a kinematic viscosity of 5.28 cSt at 100 °C is ≈ 180 ppm, dependent on temperature [12], which agrees with the findings in this paper for fully formulated oil. In theory, the reduction in viscosity causes the contacts lambda ratio to reduce, which could potentially influence the formation. Previous research has shown that an increase in oil viscosity with low Mo concentration impacts friction at lambda ratios ranging from 0.1 to 0.3 [34]. However, regardless of oil viscosity, higher Mo concentrations are impacted less. To fully optimize the Mo concentration further in ultra-low viscosity with application to the ICE, the optimum concentration must keep low friction over varying lambda ratios as its higher concentration counterparts and a similar steady-state friction value.

3.1.2. *Coefficient of friction under varying lambda ratios*

Fig. 3-4 displays the final Stribeck curves obtained at 20 h into the test when the steady-state friction value has been well achieved in the traction phase. The graph shows the entrainment speed where the lubrication regime transitions from boundary to mixed at 1320 mm/s. Sample with 0 ppm of Mo clearly shows the highest friction values over the whole range of entrainment speeds used. This Stribeck curve resembles recent research that tested fully formulated higher viscosity oils, 0 W-20, with no friction modifier [35]. Regardless of oil viscosity, as long as anti-wear and detergent additives are present within the fully formulated oil, an increase of steady-state friction to ≈ 0.13 will be observed. This is due to the tribofilm being composed of ZDDP and detergent products.

It is very clear from the final Stribeck curves that Mo concentrations ≥ 350 ppm all exhibit similar friction behavior. The Stribeck curves for these concentrations, where the friction ≈ 0.04 does not fluctuate with lambda ratio changes in the boundary and mixed regimes, are typical for fully formulated oils with high Mo concentrations [36,37].

The attention of analysis on the graph must be given to the 180 ppm

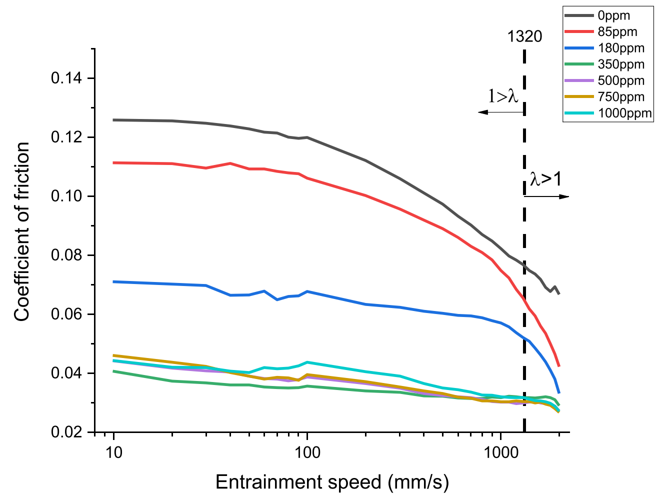

Fig. 3-4. Final Stribeck curves for all Mo concentrations.

of Mo sample oil. In the previous section, 180 ppm produced a steady-state friction value at a constant lambda ratio of ≈ 0.04. However, under varying lambda ratios, it is clear that the low friction value of ≈ 0.04 is unattainable. The Stribeck curves taken at every interval for

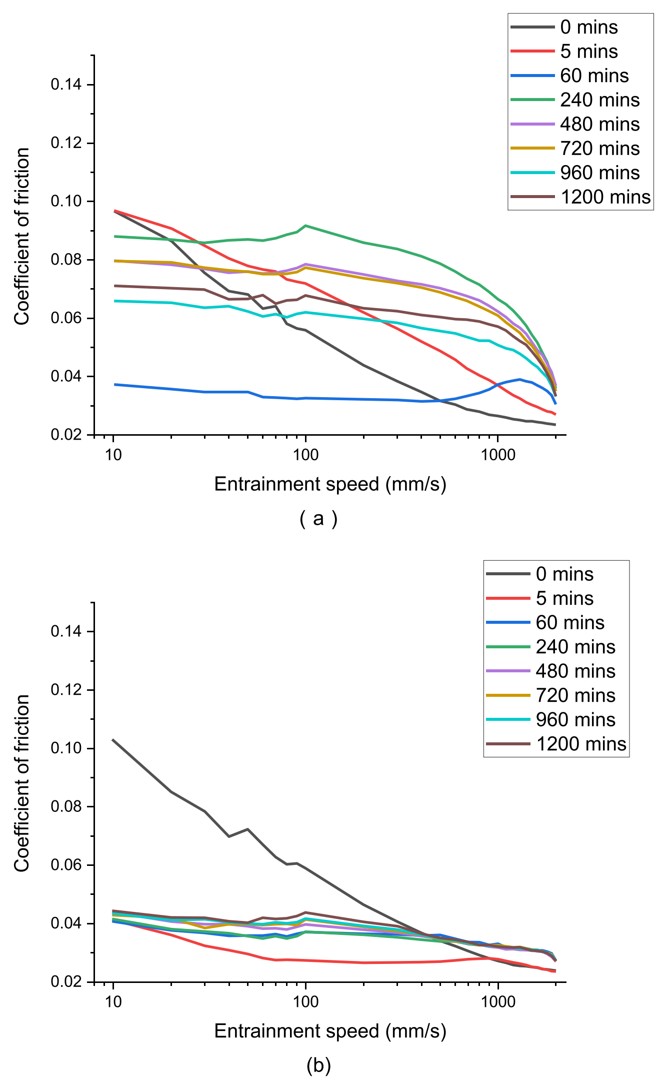

Fig. 3-5. Stribeck curves (a) 180 ppm of Mo and (b) 1000 ppm of Mo.

the 180 ppm concentration are shown in part (a) of Fig. 3-5. For comparison, the 1000 ppm concentration is also included in part (b) of Fig. 3-5. Higher friction values are obtained across the whole range of entertainment speeds for 180 ppm than higher Mo concentrations. This shows the importance of testing fresh oils under varying lambda ratios along with a constant lambda ratio. A concentration greater than 180 ppm can keep a low friction value of ≈ 0.04 under the varying lambda ratios. The theory for why the tribofilm and Mo concentration at 180 ppm produces increased friction under a varying lambda ratio can be explained using tribofilm characterization techniques, shown later.

3.1.3. Induction time

Another factor to consider when investigating the optimum Mo concentration for ultra-low viscosity engine oils is the time for the friction to reduce to its steady-state value of ≈ 0.04.

The induction time to reach each Mo concentration steady-state value is shown in Fig. 3-6. Steady-state friction is determined by averaging the friction in the traction phase towards the end of the test, as shown in Fig. 3-2. Only the Mo concentrations, which reduced the friction to ≈ 0.04, are included. Standard deviations for the repeated tests are also included. Again, a clear trend is observed; increasing the Mo concentration decreases the induction time to reach its steady-state friction value. The induction time reduction with higher concentration can be explained by the formation and removal of MoS_2 in the tribofilm matrix. Previous research determined that in the initial stages of the rubbing period, the tribofilm matrix is very thin with amorphous MoS_2 structures dispersed. As the surfaces continue to rub, the tribofilm matrix becomes thicker with a layer-lattice structure of MoS_2, which leads to friction reduction and an induction time. At that point in the tribofilm formation, the formation rate of MoS_2 is greater than the removal rate [28]. Clearly from Fig. 3-6, increasing the Mo concentration decreases the induction time to reach a steady-state friction value. Mo concentration must be a significant contributor to the formation rate of MoS_2, which increases the imbalance between the formation and removal rate as Mo concentration increases. When the formation rate of MoS_2 becomes more significant at the initial tribofilm formation, the induction time decreases. In theory, more and thicker MoS_2 layers are formed within the MoDTC/ZDDP tribofilm matrix in the initial stages of the tribofilm formation. Once the rate of formation is equal to the rate of removal, steady-state friction is achieved. Increasing the Mo concentration greater than 1000 ppm will further decrease the induction time. However, there should be a maximum Mo concentration to which further increases do not reduce the induction time. This concentration would be a lot greater than 1000 ppm.

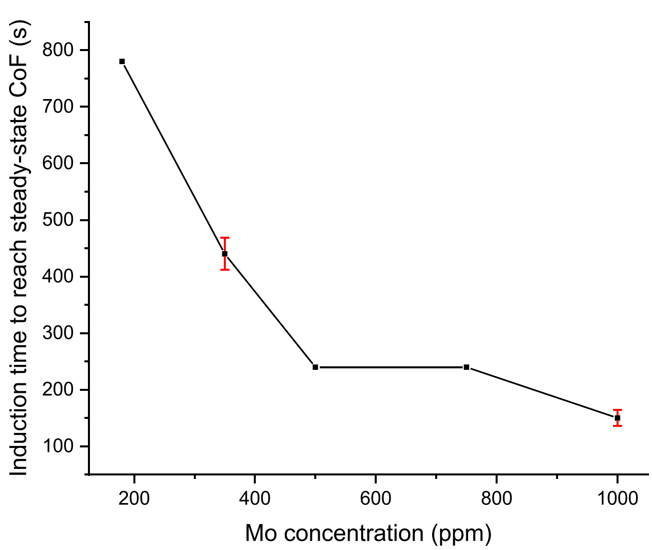

Fig. 3-6. Induction time to reach a steady-state friction value of 0.04.

After each Stribeck phase has occurred, there is also an induction period for the coefficient of friction to reach its steady-state value. To highlight the influence Mo concentration has on this induction period, 180, 350, and 1000 ppm sample oils first 500 s of traction after Stribeck curves are shown in Fig. 3-7.

Part (a) of Fig. 3-7, for 180 ppm, clearly shows that the friction value in the traction phase has to decrease after the Stribeck curve phases have been completed. The Stribeck curves varying lambda ratio and entrainment speed create instability in the tribofilm matrix, increasing the friction when the contact is constant, mainly due to very low lambda ratios used in the Stribeck curve, much lower than in the traction phase. Regardless of test time, there is still an induction period for the friction to reach its steady-state value again. Once the Mo concentration is increased to 350 ppm, part (b) of Fig. 3-7, the friction after the Stribeck curve phase at the start of the traction is lower, and the induction time decreases, suggesting a more stable tribofilm matrix, with the ability to keep low friction. Again when increasing the Mo concentration to 1000 ppm, the same effect is observed, part (c) of Fig. 3-7. Therefore, Mo concentration significantly influences the friction function of the tribofilm matrix well after steady-state friction and full tribofilm formation has occurred.

3.2. Tribofilm thickness

Optical film thickness measurements using the SLIM technique are critical to understanding the influence Mo concentration has on the growth of the tribofilm and steady-state film thickness values. Three of the Mo concentration were selected for friction test repeats with the SLIM. 0 ppm, 350 ppm, and 1000 ppm. The selections were based on the friction analysis from the initial tests.

3.2.1. Tribofilm growth rate and steady-state film thickness

Fig. 3-8 displays the optical film thickness growth for the selected Mo concentrations during the test duration. The SLIM images for the final measurement towards the end of the test are also shown on the graph's right-hand side.

The 0 ppm of Mo test shows a steady-state optical film thickness of ≈ 110 nm, typical of tribofilms which mainly consist of the ZDDP products such as zinc sulfide, glassy phosphates, and zinc polyphosphate chains formed during rubbing [29]. The addition of MoDTC into the oil, which is sufficient to reduce the friction to ≈ 0.04, clearly shows a decrease in steady-state optical film thickness. The decrease observed when adding MoDTC can be explained by the competitive absorption between the boundary-active additives [38]. The theory suggests that MoDTC prevents the complete formation of a ZDDP tribofilm. Since a fully formed MoDTC tribofilm is only ≈ 10–20 nm thick, the general film thickness decreases in fully formulated oil [22].

Since the SLIM technique favors ZDDP tribofilms and it has been determined from previous research that MoS_2 produces a tribofilm thickness which produces immeasurable results, it becomes difficult to determine the thickness of the MoS_2 part of the tribofilm matrix in the beginning stages of the test [20,29]. However, from the results, the ZDDP thickness does decrease with the addition of MoDTC, indicated by the light brown colors and values. Increasing the Mo concentration from 350 to 1000 ppm does not significantly change the steady-state film thickness values. The difference between the Mo concentrations is the tribofilm growth rate. After 5 min of traction, 350 ppm of Mo has a slightly thicker tribofilm than 1000 ppm, suggesting a thicker ZDDP part of the tribofilm with MoS_2 formed within.

3.3. Tribofilm chemical composition

To further understand the differences between the 180 and 350 ppm of Mo tribofilms, XPS analysis has been utilized to determine the species associated with certain additives. At the same time, Raman enabled the analysis of MoS_2 in terms of coverage and peak intensity within the

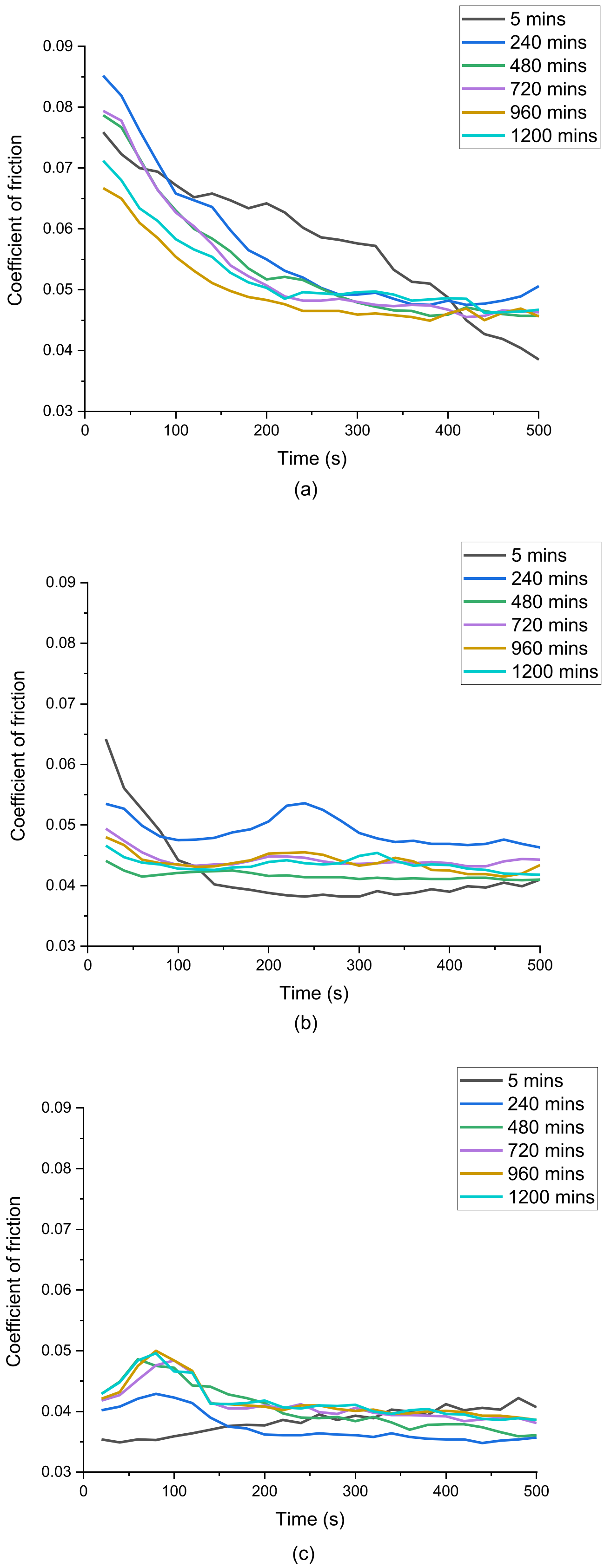

Fig. 3-7. Induction period after Stribeck curves for (a) 180 ppm, (b) 350 ppm and (c) 1000 ppm.

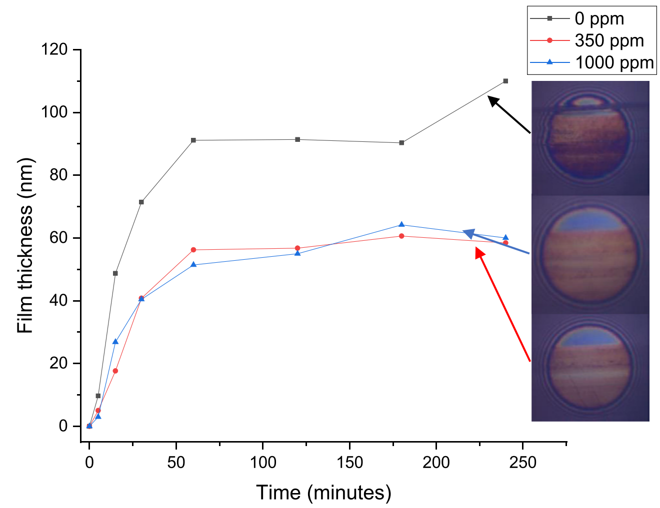

Fig. 3-8. Optical film thickness for 0, 350 and 1000 ppm of Mo tribofilms.

tribofilm to accompany the XPS data.

3.3.1. *X-ray Photoelectron Spectroscopy*

Fig. 3-9 displays the Mo3d deconvoluted XPS signals at 0 and 120 s etch time for samples with 180 and 350 ppm of Mo. All Mo concentrations higher than 350 ppm produced the same peaks as 350 ppm at 0 and 120 s etching time.

Peaks at S2s and two chemical states of Mo at (IV) and (VI) were detected at 0 s etch time for both samples. This suggests that at 0 s etch time for both tribofilms, metal sulfide from the S 2 s peak and MoS_2 and Mo oxides from Mo (IV) and Mo (VI) are present. Peaks detected at 0 s are typical of tribofilms with Mo species decomposed from MoDTC in fully formulated oils [25,38–40]. The difference between the two HR scans at 0 s etch time is the Mo (IV): Mo (VI) ratios. At 0 s etching time, the Mo (IV): Mo (VI) ratio for 180 ppm is 53.45: 13.38 and 70.07: 8.71 for 350 ppm. Previous research has shown that Mo (IV): Mo (VI) ratios can be used to analyze the MoS_2 to Mo oxides ratio to understand the Mo species formed from MoDTC in terms of quantity [25,31]. A higher Mo (IV): Mo (VI) ratio indicates a higher concentration of MoS_2 than Mo oxides in the tribofilm. It must be noted that the Mo concentrations greater than 350 ppm all produced similar ratios compared to 350 ppm at 0 s etching time. Similar ratios indicate that an increase in Mo concentration past the critical concentration does not affect the concentration of MoS_2 compared to Mo oxides at 0 s etch time. Therefore, XPS and tribofilm thickness analysis suggest tribofilm chemistry and thickness do not significantly change when increasing the Mo concentration past the critical concentration, 350 ppm.

The peaks within the 120 s etching time signals show significant differences between the two concentrations. 180 ppm produces a weak signal which can not be analyzed, suggesting no Mo species are present at 120 s etching time. 350 ppm has the same peaks at 120 s etching time compared to 0 s with additional peaks associated with Mo (V) chemical state. The additional Mo (V) chemical state peak is associated with Mo oxysulphide [40]. For all Mo concentrations $\geq$ 180 ppm, the Mo (IV): Mo (VI) ratios decrease as the etching time increases from 0 to 120 s. No peak detection at 120 s for 180 ppm suggests Mo species are more embedded within the layers towards the substrate for 350 compared to 180 ppm.

3.3.2. *Raman spectroscopy*

Fig. 3-10 displays the Raman mapping and frequency distribution of intensity for the 180 and 350 ppm tribofilms to accompany the XPS analysis. XPS has shown that 350 ppm of Mo has more MoS_2 species at 0 and 120 s etch time, suggesting more MoS_2 is embedded within the ZDDP dominant tribofilm. While tribofilm thickness has shown, ZDDP

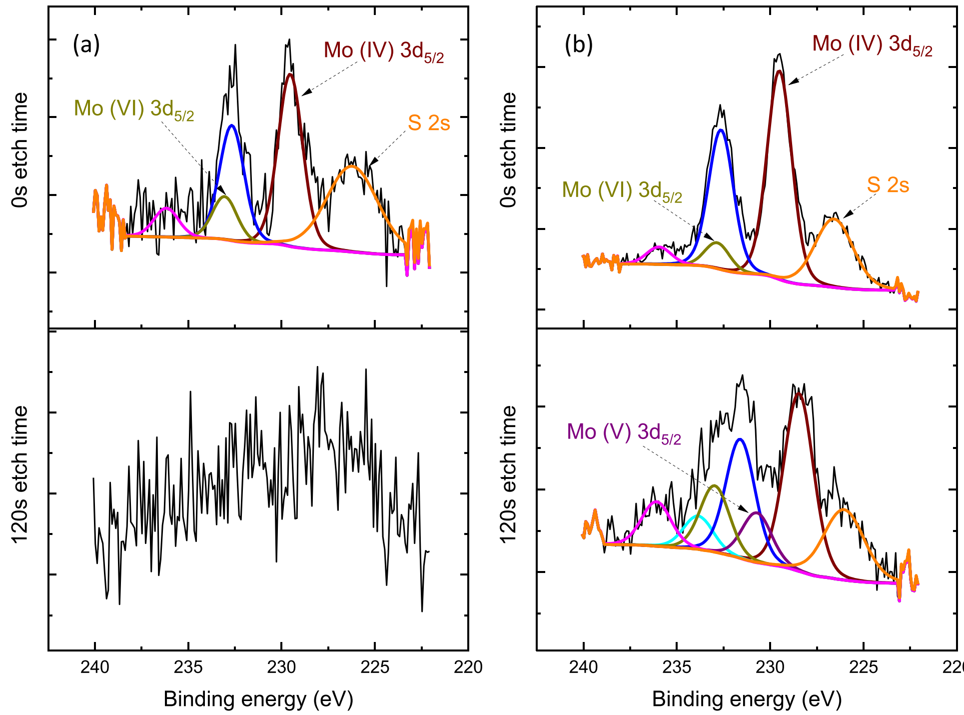

Fig. 3-9. XPS analysis for Mo 3d signal at 0 and 120 s etch times (a) 180 ppm and (b) 350 ppm.

dominated tribofilms decrease in thickness with the addition of MoDTC, and an increase of Mo concentration greater than 350 ppm does not significantly change the steady-state film thickness.

Apparent differences can be seen between the Raman mapping and peak intensity frequency of the 180, 350, and 1000 ppm tribofilms. 180 ppm has less MoS_2 coverage than 350 ppm with lower total intensity counts. The majority of the higher intensity areas are found within the center of the tribofilm for 180 and 350 ppm. Once the concentration increases past 500 ppm, the intensity areas cover larger areas of the tribofilm, as shown in Fig. 3-10 for 1000 ppm. Previous research also found that the higher intensity areas of MoS_2 were towards the center of the Hertzian contact pressure point for a 500 ppm of Mo fully formulated engine oil [41]. However, the operating conditions were less harsh than those used in this study. The total count for 180 ppm tribofilms is ≈ 50% less than 350 ppm. The coverage does not increase as the Mo concentration increases past 350 ppm. However, the total intensity counts and peak intensity frequency increase to a maximum point, as shown in Fig. 3-11.

The maximum total intensity counts and peak intensity occur when the Mo concentration is ≥ 500 ppm, with ≈ 30–50% higher total intensity counts than 350 ppm's tribofilm, outlined in Fig. 3-10 and Fig. 3-11. An increase in total intensity counts MoS_2 within the tribofilm as Mo concentration increases have been documented in previous research, but only with two different Mo concentrations [34]. Once the Mo concentration is increased past 500 ppm, the Mo concentration does not impact the total intensity counts and coverage of MoS_2 within the ZDDP dominate tribofilm. However, a slight decrease in friction is observed with concentrations greater than 500 ppm. The increase in total intensity counts and full coverage within the tribofilm matrix can explain this.

The XPS, Raman data, and analysis findings coupled with the tribofilm thickness results can explain the increased friction in the Stribeck curves for 180 compared to 350 ppm of Mo. It takes roughly 13 min of traction at a constant speed for 180 ppm of Mo to reduce the friction to ≈ 0.04, which suggests that around this point in the test, MoS_2 layers are relatively thick in the MoDTC/ZDDP/detergent tribofilm matrix. Previous research has shown that reaching a friction value of ≈ 0.04 requires thick MoS_2 layers within the tribofilm matrix [28]. The XPS and Raman data suggest that Mo concentration significantly influences the thickness of MoS_2 layers within the tribofilm matrix and the Stribeck curve friction is highly dependent upon it. However, past a threshold concentration, the thickness of MoS_2 layers is a lot less significantly impacted. The destructive nature of rapidly changing lambda ratios in the Stribeck phase removes part of the tribofilm. As part of the tribofilm is removed, the MoS_2 within the tribofilm reduces significantly for 180 ppm, shown in Fig. 3-9 and Fig. 3-10. As Mo concentration increases, the effect this has on the friction is lowered, Fig. 3-7. Therefore, 180 ppm does not produce a MoDTC/ZDDP/detergent tribofilm matrix with thick enough MoS_2 layers to keep a reduced friction value of ≈ 0.04 when the lambda ratio changes from constant to varying. The friction also fluctuates under a constant speed, as shown in Fig. 3-2. Once the constant lambda ratio is resumed after the Stribeck curve phase, the MoS_2 layers removed reform in the tribofilm matrix to obtain the ≈ 0.04 friction. This process is constantly repeated should the tribofilm thickness or operating conditions change.

3.4. Wear analysis

The optimum Mo concentration for new ultra-low viscosity engine oils must not negatively impact the wear of the tribocontacts. Wear and friction are the two most important factors that determine where the Mo concentrations optimum value is. Therefore, there must be a balance between low friction and low wear. After completing the friction tests and analysis, three Mo concentrations were selected for wear analysis. The sample with no Mo, the sample with the lowest concentration producing the same results as its higher concentration counterparts, and the higher Mo concentration tested.

3.4.1. Wear coefficients

Fig. 3-12 displays the wear coefficients calculated from wear volume loss values and the average wear scar widths obtained from an optical microscope. Both sets of results are in agreeance with each other.

From the results, adding MoDTC into a fully formulated oil increases the wear coefficient and average wear scar width. Recent research also

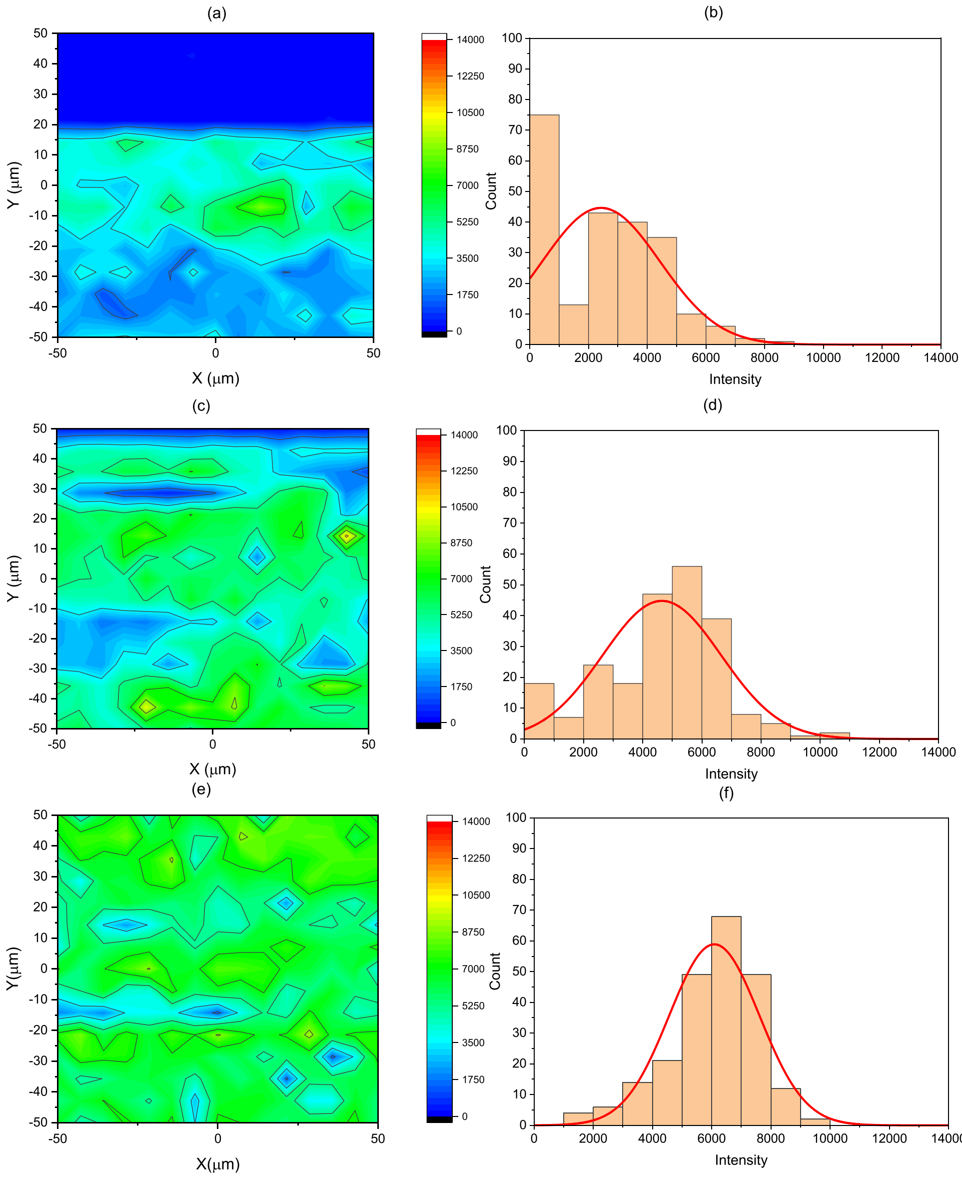

Fig. 3-10. Fig. 3 11 Raman mapping and peak intensity frequency for 180 ppm (a) mapping area, (b) intensity frequency, 350 ppm (c) mapping area, (d) intensity frequency and 1000 ppm (e) mapping area, (f) intensity frequency.

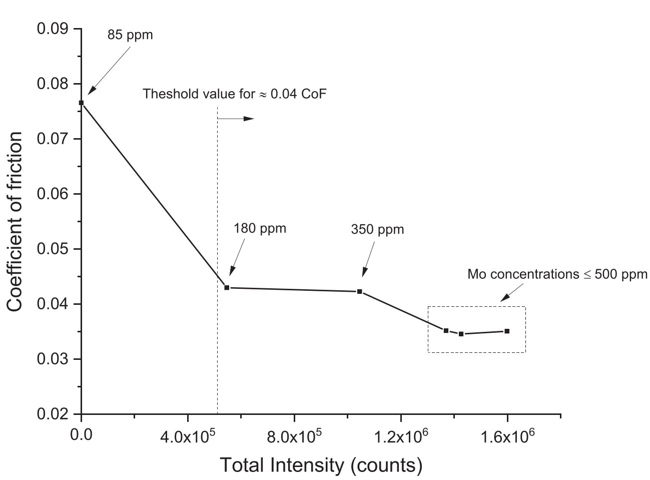

Fig. 3-11. Total intensity counts of MoS2 vs friction for all friction reducing Mo concentrations.

agrees with this statement [35]. The authors found that wear generated when using a 0 W-20 engine oil with 250 ppm of Mo in the form of MoDTC produces a 48% increase compared to the same fully formulated engine oil without MoDTC present. Again, this can be explained by additive competitive absorption between ZDDP and MoDTC. Other research into the anti-wear performance of organomolybdenum compounds as lubricant additives found that when testing 15 W-30 engine oils, the addition of MoDTC did not improve the wear performance [42]. Therefore, regardless of oil viscosity, adding MoDTC into a fully formulated oil increases the wear and decreases the anti-wear properties of the oil. However, it must be noted that the new wear generated from adding MoDTC into the formulated oils is still low. As a system, the addition of ≈ 350 ppm's ability to keep low friction and low wear outweighs the lower wear observed with no MoDTC with higher friction.

Increasing the Mo concentration from 350 to 1000 ppm displays a slight decrease in wear generated. However, in real-world applications such as the ICE, the difference in wear between the two Mo concentrations is negligible. Therefore, increasing the Mo concentration by ≈ 180% and not negatively impacting the wear is positive. In theory, increasing the Mo concentration much higher than 1000 ppm could

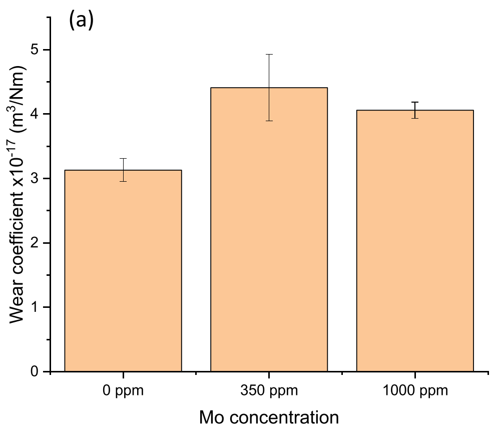

(b)

The concentration of Mo (ppm)	Average wear scar width (µm) – optical microscope
0	144.48
350	149.83
1000	147.83

Fig. 3-12. (a) Wear coefficients and (b) average wear scar width from optical microscope images.

negatively impact the wear, preventing ZDDP formation.

4. Conclusions

This paper has investigated the optimization of Mo concentration in new ultra-low fully formulated fresh engine oils. The resulting conclusions drawn from this research paper are;.

- The critical Mo concentration for new ultra-low engine oil in this research is between 180 and 350 ppm in fresh engine oil.
- Mo concentrations $\geq$ 350 ppm up to 1000 ppm do not negatively impact the friction or wear of the tribo-contact. However, concentrations much higher than 1000 ppm could potentially result in negative wear data.
- Increasing the Mo concentration within fully formulated oil decreases the induction time to a steady-state friction value of $\approx$ 0.04, which increases the MoS_2 layer thickness in the ZDDP dominant tribofilm in the beginning stages of film formation.
- The rate of formation and removal of MoS_2 within a ZDDP dominant tribofilm is highly dependent on Mo concentration, and the formation rate becomes more significant with increased Mo concentration.
- Increasing the Mo concentration increases the total intensity counts of MoS_2 within the tribofilm. However, once a threshold concentration is reached, in this study, 500 ppm, the value does not significantly change, suggesting MoS_2 layer thickness has a threshold.
- Optical film thickness decreases significantly with the addition of MoDTC. However, increasing the Mo concentration greater than the critical concentration does not change the tribofilm steady-state value.
- Adding MoDTC into a fully formulated oil increases the wear generated due to competitive surface absorption. However, increasing the Mo concentration greater than the critical concentration does not negatively impact the wear generated, and the differences are negligible.

CRediT authorship contribution statement

Aaron Thornley: Conceptualization, Methodology, Formal analysis, Investigation, Data Curation, Writing - Original Draft, Writing - Review & Editing, Visualization. **Yuechang Wang**: Supervision, Writing - Review & Editing, Validation, Visualization. **Chun Wang**: Supervision, Investigation, Data curation, Writing - Review & Editing. **Jiaqi Chen**: Resources, Investigation, Writing - Review & Editing. **Haipeng Huang**: Resources, Investigation, Writing - Review & Editing. **Hong Liu**: Resources, Writing - Review & Editing, Project administration. **Anne Neville**: Supervision, Funding acquisition, Project administration. **Ardian Morina**: Supervision, Writing - Review & Editing, Project administration.

Declaration of Competing Interest

The authors declare that they have no known competing financial interests or personal relationships that could have appeared to influence the work reported in this paper.

Acknowledgments

The funding was provided by the Engineering and Physical Sciences Research Council (EPSRC), EPSRC Centre for Doctoral Training in Integrated Tribology. Grant No. EP/L01629X/1. The authors want to also acknowledge the supply of the sample oils by the Sinopec Lubricant Company.

References

[1] National Highway Transportation Administration [Internet]. Available from: ⟨https://www.nhtsa.gov/⟩.
[2] United States Enviromental Protection Agency. Available from: ⟨https://www.epa.gov/⟩.
[3] Mock P. Emission Standards for Passenger Cars and Light-Commercial Vehicles in the European Union. ICCT Policy Updat [Internet]. 2019;(January 2019). Available from: ⟨http://www.europarl.europa.eu/news/en/press-room/20181218IPR22101/curbing-co2⟩-.
[4] Inoue K, Tominaga E, Akiyama K, Ashida T. Effects of lubricant composition on fuel efficiency in modern engines. SAE Trans 1995:728–36.
[5] Tanaka H, Nagashima T, Sato T, Kawauchi S. The effect of 0W-20 low viscosity engine oil on fuel economy. SAE Tech Pap Ser, 1; 2010. 724.
[6] Mufti RA, Priest M. Effect of engine operating conditions and lubricant rheology on the distribution of losses in an internal combustion engine. J Tribol 2009;131(4).
[7] Okuda S., Saito H., Nakano S., Koike Y. Development of JASO GLV-1 0W-8 Low Viscosity Engine Oil for Improving Fuel Efficiency considering Oil Consumption and Engine Wear Performance. 2020;1–9.
[8] Yamamori K., Uematsu Y., Manabe K., Miyata I., Motor T., Kusuhara S. Development of Ultra Low Viscosity 0W-8 Engine Oil. 2020;1–7.
[9] Anderson WB, Guinther GH. Engine oil fuel economy: benefits and potential debits of low viscosity engine oil. SAE Tech Pap Ser. 2019. p. 1.
[10] Bovington C, Korcek S, Sorab J. The importance of the Stribeck curve in the minimisation of engine friction. Tribol Ser 1999;36:205–14.
[11] Graham J, Spikes H, Jensen R. The friction reducing properties of molybdenum dialkyldithiocarbamate additives: part ii - durability of friction reducing capability. Tribol Trans 2001;44(4):637–47.
[12] Graham J, Spikes H, Korcek S. The friction reducing properties of molybdenum dialkyldithiocarbamate additives: part i — factors influencing friction reduction. Tribol Trans 2001;44(4):626–36.
[13] Spikes H. The history and mechanisms of ZDDP. Tribol Lett 2004;17(3):469–89.
[14] Martin JM, Onodera T, Minfray C, Dassenoy F, Miyamoto A. The origin of anti-wear chemistry of ZDDP. Faraday Discuss 2012;156:311–23.
[15] De Feo M, Minfray C, De Barros Bouchet MI, Thiebaut B, Martin JM. MoDTC friction modifier additive degradation: correlation between tribological performance and chemical changes. RSC Adv 2015;5(114):93786–96. https://doi.org/10.1039/C5RA15250J.
[16] Yan L, Yue W, Wang C, Wei D, Xu B. Comparing tribological behaviors of sulfur- and phosphorus-free organomolybdenum additive with ZDDP and MoDTC. Tribol Int 2012;53:150–8.

[17] Spikes H. Low-and zero-sulphated ash, phosphorus and sulphur anti-wear additives for engine oils. Lubr Sci 2008;20(2):103–36.
[18] Shimizu Y, Spikes HA. The Influence of Slide–Roll Ratio on ZDDP Tribofilm Formation. Tribol Lett 2016;64(2):1–11.
[19] Lubrecht AA, Venner CH, Colin F. Film thickness calculation in elasto-hydrodynamic lubricated line and elliptical contacts: the Dowson, Higginson, Hamrock contribution. Proc Inst Mech Eng Part J J Eng Tribol 2009;223(3):511–5.
[20] Khaemba DN. Raman spectroscopic studies of friction modifier Molybdenum DialkyldiThioCarbamate (MoDTC). 2016.
[21] Luiz JF, Spikes H. Tribofilm formation, friction and wear-reducing properties of some phosphorus-containing anti-wear additives. Tribol Lett 2020;68(3):1–24. https://doi.org/10.1007/s11249-020-01315-8.
[22] Okubo H, Tadokoro C, Sasaki S. In situ raman-SLIM monitoring for the formation processes of MoDTC and ZDDP tribofilms at Steel/Steel contacts under boundary lubrication. Tribol Online 2020;15(3):105–16.
[23] Elinski MB, LaMascus P, Zheng L, Jackson A, Wiacek RJ, Carpick RW. Correction to: "Cooperativity between zirconium dioxide nanoparticles and extreme pressure additives in forming protective tribofilms: toward enabling low viscosity lubricants". Tribol Lett 2021;69(4):140. https://doi.org/10.1007/s11249-021-01510-1.
[24] Soltanahmadi S, Morina A, Van Eijk MCP, Nedelcu I, Neville A. Investigation of the effect of a diamine-based friction modifier on micropitting and the properties of tribofilms in rolling-sliding contacts. J Phys D Appl Phys 2016;49(50):505302.
[25] Komaba M, Kondo S, Suzuki A, Kurihara K, Mori S. The effect of temperature on lubrication property with MoDTC-containning lubricant —temperature dependence of friction coefficient and tribofilm structure—. Tribol Online 2018;13(5):275–81.
[26] Thornley B, Beadling R, Bryant M, Neville A. Investigation into the repassivation process of CoCrMo in a simulated biological environment. Corrosion 2020;76(6):539–52.
[27] Khaemba DN, Neville A, Morina A. A methodology for Raman characterisation of MoDTC tribofilms and its application in investigating the influence of surface chemistry on friction performance of MoDTC lubricants. Tribol Lett 2015;59(3):1–17.
[28] Xu D, Wang C, Espejo C, Wang J, Neville A, Morina A. Understanding the friction reduction mechanism based on molybdenum disulfide tribofilm formation and removal. Langmuir 2018;34(45):13523–33.
[29] Topolovec-Miklozic K, Forbus TR, Spikes HA. Film thickness and roughness of ZDDP anti-wear films. Tribol Lett 2007;26(2):161–71.
[30] Espejo C, Thiébaut B, Jarnias F, Wang C, Neville A, Morina A. MoDTC tribochemistry in steel/steel and steel/diamond-like-carbon systems lubricated with model lubricants and fully formulated engine oils. J Tribol 2019;141(1):1–12.
[31] Komaba M, Kondo S, Suzuki A, Kurihara K, Mori S. Kinetic study on lubricity of MoDTC as a friction modifier. Tribol Online 2019;14(4):220–5.
[32] Rai Y, Neville A, Morina A. Transient processes of MoS2 tribofilm formation under boundary lubrication. Lubr Sci 2016;28(7):449–71.
[33] Greenall A, Neville A, Morina A, Sutton M. Investigation of the interactions between an ovel, organic anti-wear additive, ZDDP and overbased calcium sulphonate. Tribol Int 2012;46(1):52–61. https://doi.org/10.1016/j.triboint.2011.06.016.
[34] Vaitkunaite G, Espejo C, Wang C, Thiébaut B, Charrin C, Neville A, et al. MoS2 tribofilm distribution from low viscosity lubricants and its effect on friction. Tribol Int 2020;151(July):106531.
[35] Moody G., Eastwood J. The performance and mechanisms of organic polymeric friction modifiers in low viscosity engine oils. 2020.
[36] Kaneko T, Yamamori K, Suzuki H, Onodera K, Ogano S. Friction reduction technology for low viscosity engine oil compatible with LSPI prevention performance. SAE Tech Pap. 2016. 2016–01-2276.
[37] Liu H, Jin J, Li H, Yamamori K, Kaneko T, Yamashita M, et al. 0W-16 fuel economy gasoline engine oil compatible with low speed pre-ignition performance. SAE Int J Fuels Lubr 2017;10. 2017-01-2346.
[38] Costello MT, Urrego RA. Study of surface films of the ZDDP and the MoDTC with crystalline and amorphous overbased calcium sulfonates by XPS. Tribol Trans 2007;50(2):217–26.
[39] Sgroi M, Gili F, Mangherini D, Lahouij I, Dassenoy F, Garcia I, et al. Friction reduction benefits in valve-train system using IF-MoS2 added engine oil. Tribol Trans 2015;58(2):207–14.
[40] Deshpande P, Minfray C, Dassenoy F, Le Mogne T, Jose D, Cobian M, et al. Tribocatalytic behaviour of a TiO2 atmospheric plasma spray (APS) coating in the presence of the friction modifier MoDTC: a parametric study. RSC Adv 2018;8(27):15056–68. https://doi.org/10.1039/C8RA00234G.
[41] Barnes AL, Morina A, Andrew RE, Neville A. The effect of additive chemical structure on the tribofilms derived from varying molybdenum-sulfur chemistries. Tribol Lett 2021;(4):69. https://doi.org/10.1007/s11249-021-01493-z.
[42] Feng X, Jianqiang H, Fazheng Z, Feng J, Junbing Y. Anti-wear performance of organomolybdenum compounds as lubricant additives. Lubr Sci 2007;19(2):81–5.